Single Stage Faraday Accelerator with Radio-frequency Assisted Discharge (SS-FARAD)

IEPC-2011-220

Presented at the 32nd International Electric Propulsion Conference, Wiesbaden, Germany September 11–15, 2011

Matthew S. Feldman* and Edgar Y. Choueiri†
Princeton University, Princeton, NJ, 08544, USA

An RF-assisted, pulsed, electrodeless accelerator concept that utilizes a single antenna coil for plasma generation and electromagnetic acceleration is presented. This concept eliminates the need for a separate ionization stage and applied magnetic fields as seen in previous Faraday Accelerator with Radio-frequency Assisted Discharge thrusters, which leads to a lighter, more compact device. Challenges in design arising from the combined circuitry are explored and a circuit topology is proposed and tested. An LC resonator is used to isolate the RF source from the acceleration pulse. It is shown that higher quality factor resonators ensure that less acceleration energy is lost into the RF source. Parasitic effects place an upper limit on the quality factor that can be utilized. Experimentation demonstrates that the acceleration pulse can be sufficiently isolated from the RF source without significant adverse affects on plasma generation.

Nomenclature

C_a = acceleration discharge capacitor
C_{p1} = parasitic capacitance in parallel with resonator inductor
C_{p2} = parasitic capacitance from resonator to ground
C_r = resonator capacitor
C_{t1} = series tuning capacitor
C_{t2} = shunt tuning capacitor
L_a = SS-FARAD antenna inductance
L_p = parasitic inductance associated with acceleration capacitor
L_r = resonator inductor
Q = quality factor
R_a = SS-FARAD antenna resistance
R_s = RF generator source resistance
V_c = charging voltage applied to acceleration capacitor
V_g = applied voltage seen by the RF generator during an acceleration discharge
ω_g = RF generator operating frequency

* Graduate Student, Mechanical and Aerospace Engineering Department, feldmanm@princeton.edu.
† Professor, Mechanical and Aerospace Engineering Department, Chief Scientist EPPDyL, choueiri@princeton.edu

I. Introduction

Pulsed inductive plasma accelerators are seen as a way to overcome major obstacles in other electric propulsion devices, particularly electrode erosion. The basic operation of inductive thrusters relies on an electric pulse being discharged by a capacitor through an inductive coil, which induces electromagnetic fields inside the propellant precipitating a current sheet. The current in the coil effects a blowing force on the generated current sheet, which serves to accelerate propellant away from the coil. Because these body forces are inductively coupled to the circuitry, the plasma can be effectively separated from the walls of the accelerator, thus greatly alleviating lifetime degradation associated with erosion as well as allowing propellants which are incompatible with wall materials.

The traditional Pulsed Inductive Thruster (PIT)[1,2] design relies on a large flat acceleration coil which generates a purely axial blowing force. Neutral propellant is directed to the coil surface, and the acceleration discharge pulse must breakdown the propellant before a current sheet can form. Inefficiencies develop due to the propellant drifting away from the coil before a current sheet is fully achieved. In order to compensate for this effect, PIT relies on large discharge voltages which can achieve breakdown quickly as compared to the pulse duration, which is generally microseconds in length. Additionally, PIT utilizes a large one-meter coil, which reduces the effect of propellant decoupling. With that in mind, PIT has been reported to achieve specific impulses of 8000s with efficiencies up to 50%. However, the large size and high voltage requirements of PIT imposes additional constraints making it not ideal for many mission types, which has led to efforts to reduce the size and mass of such an inductive device.

In order to improve the feasibility of these pulsed devices, Jahn[3] suggested that pre-ionizing the propellant before the acceleration pulse could yield a benefit in efficiency by reducing the time-scale over which the current sheet forms and decreasing the voltages necessary for formation. Some of the first attempts at pre-ionization on PIT-like thrusters involved a secondary, smaller capacitor being discharged through the acceleration coil just prior to the main acceleration capacitor[4]. These pre-ionization schemes generally required large voltages on the ionizing capacitor, which contributed to pushing the propellant away from the acceleration coil prior to the main pulse. The net effect of this decoupling decreased thruster efficiency notably as compared to the traditional PIT.

Recent work has examined methods to reduce the mass and size of these thrusters through a different ionization scheme. The Faraday Accelerator with Radio-frequency Assisted Discharge (FARAD) thruster concept[6] separates the propulsion scheme into two distinct stages: ionization and acceleration. The ionization stage utilizes an RF generator directing power through a second antenna designed to create an inductive discharge and form a seed plasma. The now ionized propellant must be guided to the acceleration coil surface, which is accomplished through an externally applied magnetic field generated by surrounding electromagnets[5–7]. Recent work has explored placing an ionization antenna nearer to the acceleration coil and removed the applied magnetic field[8]. Acceleration stages have been made using both flat, Marx-coils typical of PIT and conical theta pinch (CTP) coils. While initial speculation was there could be beneficial effects on thrust from the pinch effect in a CTP antenna, recent work suggests the pinch-generated thrust is small in comparison to the directed axial thrust[9]. Nevertheless, a conical antenna could still prove beneficial in an inductive thruster concept by helping to reduce fringe losses seen in PIT-like devices. Overall, the FARAD pre-ionization scheme has lead to current sheet formation with lower pulse energies and a smaller device than PIT[6].

A subsequent ionization scheme for a FARAD-like device called the Microwave Assisted Discharge Inductive Plasma Accelerator (MAD-IPA) utilizes electron cyclotron resonance (ECR)[10]. In this scheme, the energy is directed through microwave waveguides and excites resonances with electrons in the plasma with the help of an applied magnetic field. The field is constructed with permanent magnets surrounding a CTP acceleration coil, which helps generate the plasma at the coil surface.

This paper introduces a FARAD device designed to decrease size, mass, and system complexity while improving energy efficiency by utilizing a single antenna coil for both pre-ionization and acceleration. The goal is to establish the potential improvements that a Single Stage FARAD (SS-FARAD) device offers over a traditional FARAD thruster, as well as demonstrate the feasibility of SS-FARAD from a technical standpoint.

The layout for the paper will proceed as follows. In Section II, the proposed thruster architecture and motivation will be described, along with obstacles and drawbacks of a SS-FARAD device. Section III describes the circuit architecture and presents an analysis of the circuit dynamics. Finally, in Section IV, simulations of the tuning circuity and acceleration pulse are performed. Experimental results of the SS-FARAD circuit test are also presented.

II. Single-Stage FARAD Concept

The SS-FARAD thruster consists of a single CTP antenna coil through which both the ionization and acceleration pulse occur (See Fig 1). Two external circuits are connected in parallel to the SS-FARAD antenna to perform these two tasks. Neutral propellant is injected along the coil surface and is ionized via a 13.56 MHz RF generator directing power to the antenna. Though the antenna geometry is non-standard, a weak inductive discharge should be obtainable near the coil surface where EM fields are strongest with tens of watts of forward power. High plasma densities are not necessary as even a weakly ionized propellant, with ionization fraction 10^{-4}, has been seen to aid current sheet formation during the acceleration pulse.[6]. A capacitive discharge is then pulsed through the coil which induces a strong current sheet and generates a primarily axial force on the propellant. The conical antenna shape serves to confine the propellant which reduces fringe effects.

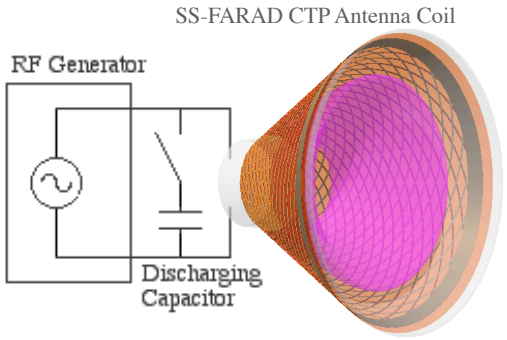

Figure 1. Simplified SS-FARAD Schematic

A. Advantages and Motivation

The SS-FARAD thruster blends the initial FARAD concept with some of the earlier attempts at pre-ionization with PIT. While it shares the main feature of acceleration via an inductive current sheet generation, it is helpful to examine the differences between SS-FARAD and previous inductive plasma accelerators with pre-ionization schemes.

- In previous FARAD thrusters, plasma is efficiently generated in a separate stage, which operates with a second antenna. In the FARAD proof of concept experiments, this stage consisted of a 6 cm diameter cylinder with an Boswell-type saddle antenna surrounding the cylinder. The SS-FARAD thruster does not utilize an ionization stage distinct from the acceleration coil, which reduces the overall size of the thruster making it an inherently more compact device. Additionally, FARAD requires an externally applied magnetic field generated through electromagnets to passively guide plasma to the acceleration coil surface. These electromagnets surround the FARAD structure further increasing its size and mass, as well as using system power to maintain the applied fields. In an SS-FARAD device, plasma is generated by the acceleration coil itself, which means the plasma is already in place for acceleration. This can generate an efficiency benefit by improving propellant coupling during the acceleration discharge as well as eliminating the need for externally applied magnetic fields, further reducing power and mass requirements.

- A recent FARAD thruster[8] has attempted to eliminate size and mass by placing the ionizing antenna surrounding the acceleration coil and removing the applied magnetic fields. The antenna geometry used for this scheme involves a ground plate directly behind a flat, Marx-type coil and a circular antenna a few centimeters axially downstream around the circumference of the thruster, creating a capacitive discharge. While this configuration similarly reduces mass and size requirements, it still adds the complexity of the second antenna with no guarantee of evenly creating a plasma across the acceleration coil surface. Additionally, this overall geometry would be difficult to implement with a conical acceleration coil.

- The MAD-IPA thruster[10] utilizes ECR, which requires microwave waveguides to direct energy into the interior volume of the conical antenna assembly. And in order to create the correct conditions for ECR, an applied magnetic field is created near the surface of the CTP antenna using an array of permanent magnets. The SS-FARAD's reliance on the CTP antenna itself for ionization eliminates the need for external structure and applied fields.

- Previous pre-ionization attempts with PIT similarly used only the acceleration coil for the ionization process. This ionization was achieved with a secondary capacitor which discharge prior to the main acceleration pulse. However, this capacitor still required large voltages to create breakdown, and these experiments demonstrated an inherent inefficiency caused as the ionization pulsed caused the propellant to drift away and decouple from the coil before the acceleration pulse began. SS-FARAD directs an RF signal through the coil, which can create breakdown at much lower voltages, thus allowing for a more compact implementation. Additionally, the lower voltage and RF oscillation should lessen any potential effects of propellant drift.

In summary, by removing the external magnetic fields, secondary antennas, and ionization stage components used in other FARAD-like devices, we create a SS-FARAD thruster which has fewer system requirements. In any space mission, a reliance on a smaller number of components leads to less failure points and an inherently more robust system.

B. Challenges for SS-FARAD Implementation

The SS-FARAD design does come with engineering challenges which must be explored prior to the construction of a thruster.

- The addition of the ionization circuitry in parallel with the acceleration capacitor can change the dynamics of the discharge waveform and jeopardize the RF generator and amplifier by subjecting it the large voltage spike. A promising solution to this is to include an LC resonator tuned to the RF frequency which acts to block the energy from the acceleration capacitor while allowing the RF signal to pass. This approach is examined in detail in the subsequent sections of the paper.

- Previous pre-ionization schemes that functioned using the acceleration coil itself suffered adverse affects on efficiency because the ionization mechanism causes the propellant to drift away and decouple from the coil. The SS-FARAD ionization scheme operates at much lower voltages which will diminish this effect. However, since ionization in the new geometry has not previously been explored, the overall structure of ionization must be characterized to ensure SS-FARAD will not suffer unintended sources of efficiency loss.

III. The SS-FARAD Circuitry

The SS-FARAD circuit schematic is shown in Fig 2. The ionization stage consists of the RF generator, a series LC resonator, and a capacitive tuning L-network. The acceleration stage consists of the acceleration capacitor, C_a, and its corresponding charging circuitry, which is not shown in the Figure. Finally, the SS-FARAD antenna is connected in parallel to both circuits and includes the antenna inductance and parasitic resistance. One might imagine that the tuning circuit capacitors could shunt energy from the acceleration discharge away from the antenna, however, in practice, the small size of the tuning capacitors prevents any significant energy loss. One might still imagine a slightly different topology wherein the resonator and tuning network locations are reversed, however, simulations described in section IV suggest the superiority of this configuration in tuning the generator signal.

This section is broken up into three parts. Part A discusses the LC resonator, which is designed to protect the RF generator from the acceleration capacitor's discharge as well as ensure the bulk of the acceleration stroke energy is delivered into the SS-FARAD antenna. Part B presents the idealized tuning circuit for the antenna, which creates an impedance match to the RF source resistance. Lastly, Part C examines the non-ideal effects of parasitic capacitance and the limitations it poses on the circuit components.

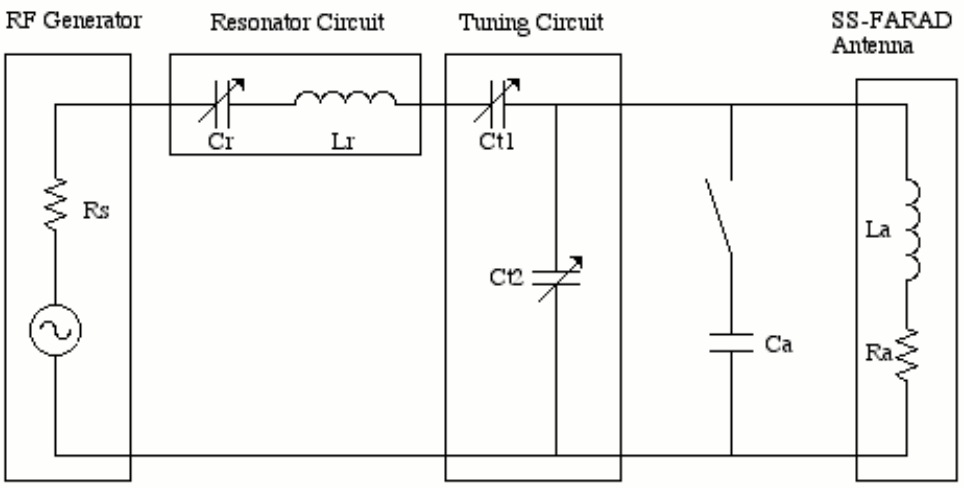

Figure 2. SS-FARAD Circuit Model. The RF Generator produces a 13.56 MHz signal with a 50Ω source resistance. The series LC resonator is tuned via a 5-500pF 3kV vacuum variable capacitor to match the 13.56 MHz signal. The tuning L-network consists of two 5-500pF air variable capacitors and acts to impedance match the SS-FARAD antenna to the generator source resistance. The acceleration capacitor is 40μF for our experiments. It is initially disconnected from the circuitry and is discharged via a hammer-activated switch. Finally, the SS-FARAD antenna has a measured inductance of 500nH and parasitic resistance on the order of .1Ω.

A. The RF Generator Protection Circuitry

The RF generator has an internal source resistance of 50 Ω and can withstand voltages on the output of up to 250 V. However, in order to protect the internal circuitry of the generator, we need to limit its operational output and ensure that the maximum externally applied voltage does not exceed 100V. This protection is accomplished via the LC resonator, which is tuned to match the RF generator frequency. The resonator will allow the generator signal to pass but will block the acceleration discharge from adversely effecting the generator. The quality factor, Q, of a resonator determines the rejection of a non-resonant signal with high Q resulting in better rejection, where

$$Q = \frac{1}{R}\sqrt{\frac{L}{C}}. \tag{1}$$

Therefore, we expect that a higher Q resonator will result in less of the acceleration discharge being seen over the RF generator

To demonstrate this, we examine analytically how the resonator reacts to the discharge. When the switch is closed, current flows from the discharge capacitor into both the SS-FARAD antenna and the choke preceding the RF generator. In order to examine the pulse seen by the generator, we assume that the time scale over which the choke dissipates the pulse is short compared to the overall timescale of the discharge capacitor acting over the antenna. This assumption is readily verified in both computer simulations and bench-top testing, which will be shown shortly. The system can therefore be simplified to a series LCR circuit with an applied constant voltage equivalent to the charge on the discharge capacitor. The simplified version of the overall circuit architecture is shown in Fig. 3. Under these conditions, the voltage seen by the generator can be found as a damped harmonic oscillator

$$\frac{d^2V_g}{dt^2} + \frac{R_s}{L_r}\frac{dV_g}{dt} + \frac{1}{L_rC_r}V_g = 0 \tag{2}$$

where the initial conditions at the start of the pulse are given by

$$V_g = 0, \frac{dV_g}{dt} = \frac{V_cR_s}{L_r} \tag{3}$$

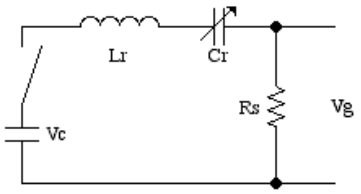

Figure 3. A simplified approximation of the RF generator protection circuitry. V_c is the voltage applied to the acceleration capacitor. V_g is the voltage seen by the RF generator over the source resistance.

where V_c is the charging voltage placed on the acceleration capacitor. For any highly underdamped oscillator, which will be true of any high Q resonator, we can approximate the maximum voltage V_g using the conservation of energy argument

$$\frac{1}{2}L_r C_r^2 \dot{V_g}^2 + \frac{1}{2}C_r V_g^2 = E_g. \tag{4}$$

Using Eqs. 3 and 4, we can calculate E_g at the initiation of the pulse:

$$E_g = \frac{V_c^2 R_s^2 C_r^2}{2L_r}. \tag{5}$$

First, we compare the energy directed through the resonator with the total energy stored in the acceleration capacitor:

$$\frac{E_g}{E_c} = \left(\frac{V_c^2 R_s^2 C_r^2}{2L_r}\right) / \left(\frac{1}{2}C_a V_c^2\right) = \frac{R_s^2 C_r^2}{L_r C_a} = \frac{1}{Q^2}\frac{C_r}{C_a}. \tag{6}$$

Next, we examine the maximum voltage seen across the generator resistor, which can be estimated from Eqs. 4 and 5 when $\dot{V}_g = 0$:

$$V_{g_{max}} = V_c R_s \sqrt{\frac{C_r}{L_r}} = \frac{V_c}{Q}. \tag{7}$$

Finally, we wish to determine the actual component size necessary to protect the RF generator from the voltage spike. The largest charging voltage used in previous FARAD proof-of-concept experiments was 2kV[6]. From Eq. 7 and the 100 V condition specified in Part A, the resonator circuit must have:

$$Q = \frac{1}{R}\sqrt{\frac{L}{C}} > \frac{V_c}{V_{g_{max}}} = 20. \tag{8}$$

Substituting for the standard LC resonance condition, $\omega_g^2 = \frac{1}{LC}$, with ω_g=13.56 MHz and rearranging, we arrive at a minimum requirement on the inductor used in the protection circuitry

$$L > \frac{V_c R_s}{V_{g_{max}}\omega_g} = 11.5\mu H, \tag{9}$$

which corresponds to a resonator capacitor of 12pF.

B. The SS-FARAD Antenna Tuning Circuit

In the FARAD Proof of Concept Experiment, the ionization antenna was tuned to the RF generator to create an impedance match with the 50Ω source resistance[5,6]. The tuning circuit consisted of a shunt-series L-network using two 1000pF vacuum variable capacitors. In SS-FARAD, a similar tuning network will be employed which matches the conical antenna to the RF generator source resistance as shown in Fig. 2. Before the switch closes activating the acceleration phase, the discharge capacitor is not connected to the RF generator or antenna and can be safely ignored in the tuning process. The generator must still act

over the LC resonator protection circuitry, but, in an ideal case, the resonator circuit will appear as zero impedance to the generator signal.

The impedance match is necessary in order to efficiently couple energy from the generator into the antenna. In a perfectly matched circuit, the forward power from the RF generator source is all directed to the antenna. Any mismatch will reflect some of the source energy, which lowers the power that reaches the propellant for ionization. However, in any efficient inductive plasma accelerator, the total energy required for ionization must be a small fraction of the acceleration pulse energy. For example, in one FARAD device[8], an ionization pulse is 0.1J compared to the acceleration pulse energy of 100J. For this reason, some mismatch in the tuning circuitry leading to power reflection can be tolerated. Reflection coefficients as much as 0.5, while not ideal, will not substantially change the performance parameters of an efficient FARAD thruster.

C. Experimental Set-Up and Non-ideal Considerations

A proof of concept of the SS-FARAD circuitry was assembled on a test bench. The acceleration capacitor used was 40μF with 36nH of parasitic inductance and was connected over a CTP antenna with approximately 500nH of inductance and on order .1Ω measured resistance. The tuning network, as described above, consisted of two 1000pF air-variable capacitors. The resonator circuit consisted of a 5-500pF 3kV vacuum variable capacitor with the ability to use various hand-wound inductors. A 13.56 Mhz signal generator was connected through an Alpha 4250 voltage standing wave ratio (VSWR)-meter to the SS-FARAD circuitry to measure tuning performance. For the acceleration discharge pulse measurements, the signal generator and VSWR-meter were replaced with a 50Ω test load over which V_g was measured. We determined that inductors wound using various magnetic cores demonstrated too much RF rejection at 13.56 MHz, which impeded the ability to tune the circuit. As a result, we wound an 11.5μH air-core solenoidal inductor to use in the resonator. This inductor's parasitic parallel capacitance was measured through it's self-resonant frequency to be no larger than 5pF.

In this set up, deviations from a perfectly matched circuit can occur in the system due to transmission line delays and parasitic effects in the LC resonator. In the ideal situation, arbitrarily larger inductances and smaller capacitances could be used in the resonator circuit until the RF generator is protected from the acceleration pulse. However, these parasitic effects can somewhat alter the acceleration pulse dynamics and can dramatically affect the load on the RF generator by altering the impedance of the resonator. The first resonator constructed was housed in a fully aluminum box, which resulted in parasitic capacitances of nearly 30pF. This dominates the 12pF calculated from Eq. 9, and the circuit could not be tuned. A second non-metallic resonator housing was constructed and demonstrated much smaller parasitic capacitances. The largest of these parasitic existed from the internal components to ground, and was measured to be approximately 5pF.

Since this value is not entirely negligible compared to the 12pF maximum value on the resonator capacitor, we used the lumped element model shown in Fig. 4 to approximate the parasitic effects.

IV. SS-FARAD Circuitry Simulations and Experimentation

A. Simulations

Due to the increased complexity generated by the parasitic capacitances, a MatLab simulation was written to examine the ability to tune a $Q = 20$ resonator circuit with the tuning configuration presented in Fig. 4. The simulation calculated the reflection coefficient for the non-ideal generator circuitry while sweeping over all possible values for the tuning capacitors. Sweeps were performed for increasing values of parasitic capacitances. A typical graph with 5pF of parasitic capacitance from the inductor to ground and the experimentally determined inductor parasitic capacitance is shown in Fig 5. The antenna is approximately tuned in the blue regions where the reflection coefficient nears 0. Further simulations demonstrate that as parasitic capacitances grows near 10pF, the circuit become untunable with the given variable capacitors. Moreover, the location and performance of the tuning region can be altered by varying the resonator capacitor from the exact resonance condition.

These simulations were repeated with the reverse circuit topology described in Section III, with varying degrees of less desirable results. In the reverse topology, even small parasitic capacitances in the resonator result in that portion of the circuitry appearing as a capacitive load, which the subsequent capacitive L-network is then incapable of tuning.

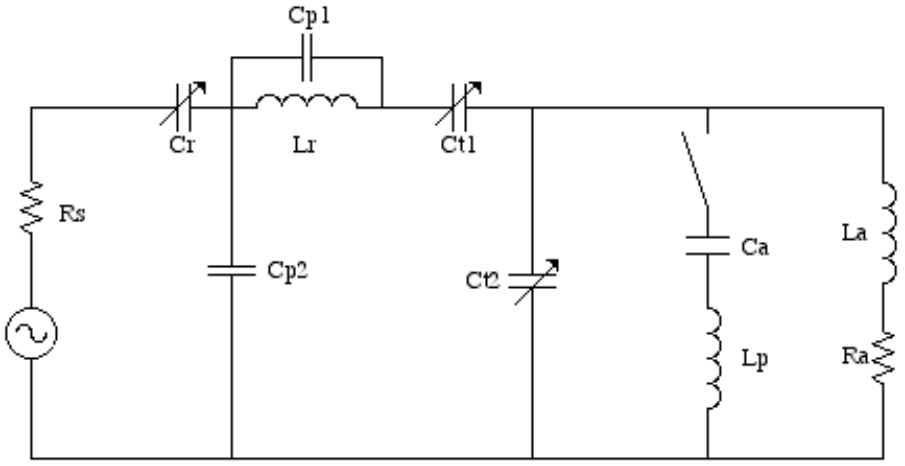

Figure 4. SS-FARAD Circuit Model with Parasitic Elements. Three parasitic elements are added to the SS-FARAD ideal SS-FARAD circuit shown in Fig. 2. C_{p1} is the parasitic capacitance in parallel with the resonator inductor. C_{p2} represents the parasitic capacitance exhibited from the resonator to ground. L_p is the parasitic inductance within the acceleration capacitor, which is approximately 36nH in the 40μF capacitor used in our experimentation.

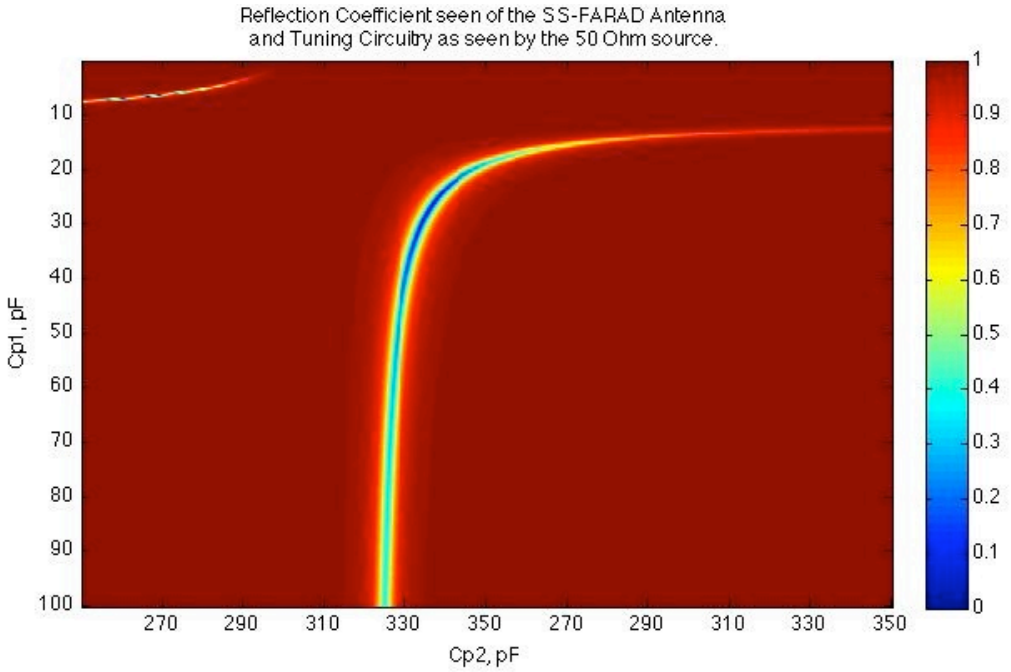

Figure 5. Reflection Coefficients while Varying Tuning Capacitances. The reflection coefficient of the SS-FARAD circuitry show in Fig. 4 is calculated for the RF generator at 13.56 MHz with respect to the 50Ω source resistance. Parasitic capacitances were approximated as 5pF. The values used for L_p and R_a were taken from experimental measurements and were 36nH and .1Ω respectively.

Before continuing with bench-top experimentation, the calculated optimal tuning capacitor values were taken from each MatLab simulation and used in a SPICE simulation of the acceleration discharge. The simulations were done assuming a 11.5μH resonator inductor with appropriate series capacitance, 5pF of parasitic capacitance, and a 40μF acceleration capacitor. The simulation also included the calculated internal inductance of the discharge capacitor which will be used in the subsequent experimentation as well as the estimated inductance and resistance of the antenna coil. Figure 6 shows a Spice simulation of the voltage seen by the RF generator in response the acceleration pulse using a $Q = 20$ resonator assuming non-ideal circuitry. Note that the maximum voltage seen is actually less than the value predicted by Eq. 7.

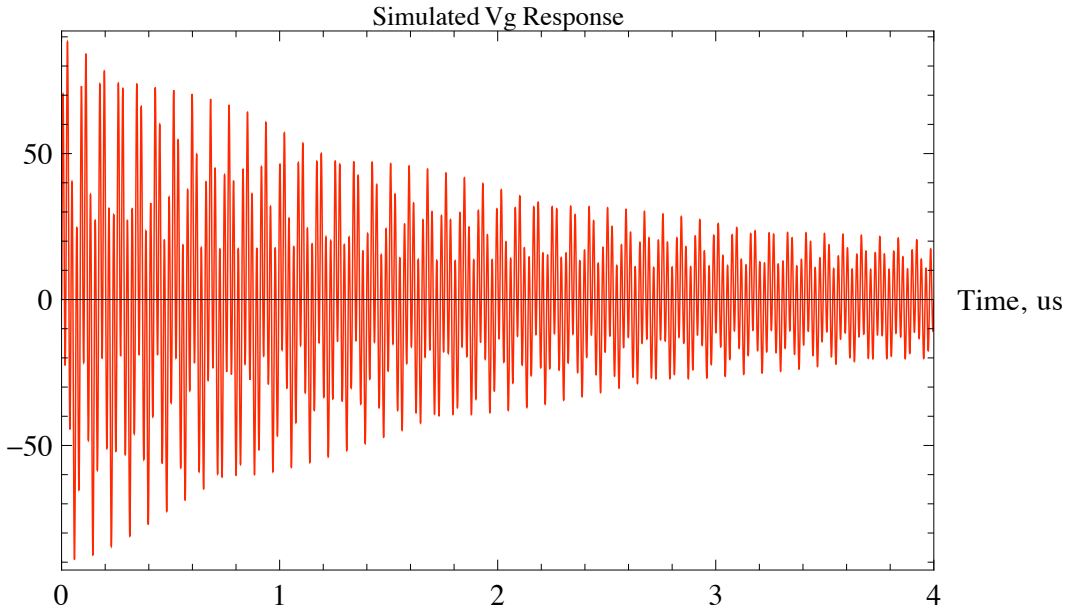

Figure 6. V_g response to a 2kV acceleration pulse using the full circuit model assuming 5pF of parasitic capacitance in a $Q = 20$ resonator. Tuning capacitor values were chosen based on the MatLab simulation in Fig. 5. The addition of parasitics and the tuning circuitry decrease the peak voltage seen to less than the predicted 100V.

Finally, we note that the initial stored energy in the acceleration capacitor is $\frac{1}{2}C_aV_c^2 = 80$J for the capacitive and charging values used in the simulations. The predicted energy lost into the generator was calculated from the simulation by numerical integration of the power dissipated through the source resistance. The total energy loss for simulation in Fig. 6 was substantially less than one mJ. Simulations for smaller Q resonators also demonstrated minimal energy loss to the generator. This finding correlates well with Eq. 6, which shows that even for small Q resonators, the small capacitors making up the supplemental RF circuitry serve to ensure that the discharge energy is deposited almost entirely into the SS-FARAD antenna, and the discharge waveform is not noticeably affected.

B. Experimental Results

Using the 11.5μH inductor, the tuning capacitors were varied and a minimum VSWR of 2.0 was achieved. This VSWR corresponds to a reflection coefficient with magnitude as low as 0.33. We then replaced the RF generator with the 50Ω test load and observed the circuit response. Initial tests were conducted charging the acceleration capacitor to 20V, instead of the 2kV expected for an actual acceleration stroke. However, due to linearity in the circuit, the maximum observed V_g should scale directly with the acceleration capacitor charging voltage. Under these conditions, the maximum observed V_g was approximately 1V, though most test runs never exceeded a 0.7V peak. A typical response of V_g and V_c is shown in Fig. 7. A zoomed in view of the generator voltage is seen in Fig. 8. While parasitics not taken into account could result in some of the distortion seen compared to the simulation in Fig. 6, the rise time associated with the V_g pulse is likely a result of the speed at which the hammer-switch activation occurs.

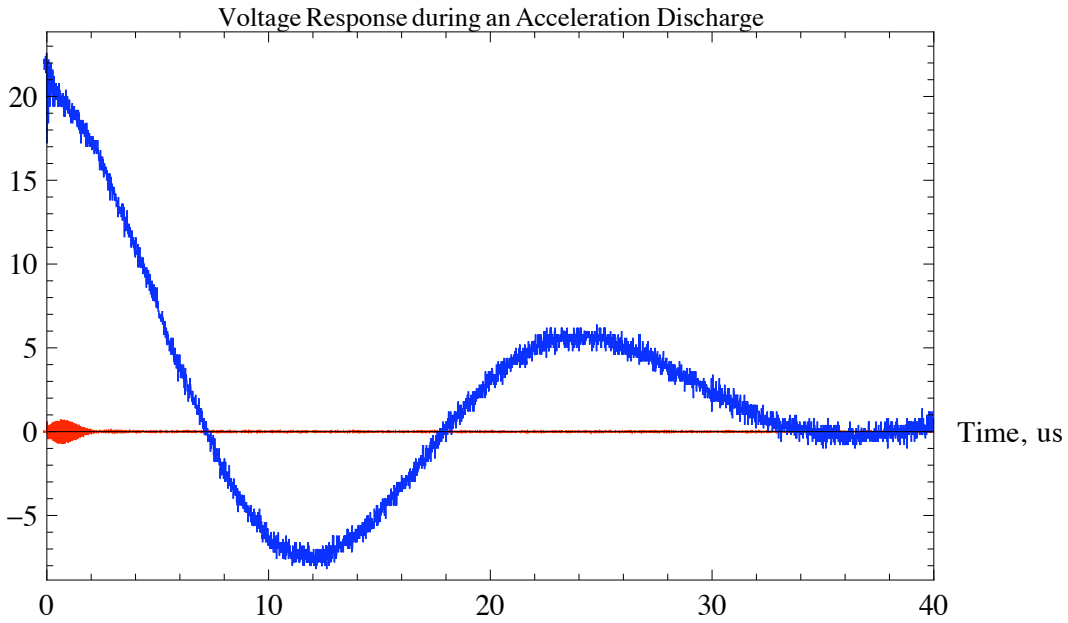

Figure 7. Voltages were measured during an acceleration discharge of the experimental test circuitry. The acceleartion capacitor was charged to 20V and its voltage over time is the blue line. The red line is the measured voltage over the 50Ω test load, which corresponds to the RF generator. The peak voltage on V_g is less than .7V, which is better performance than the predicted upper bound.

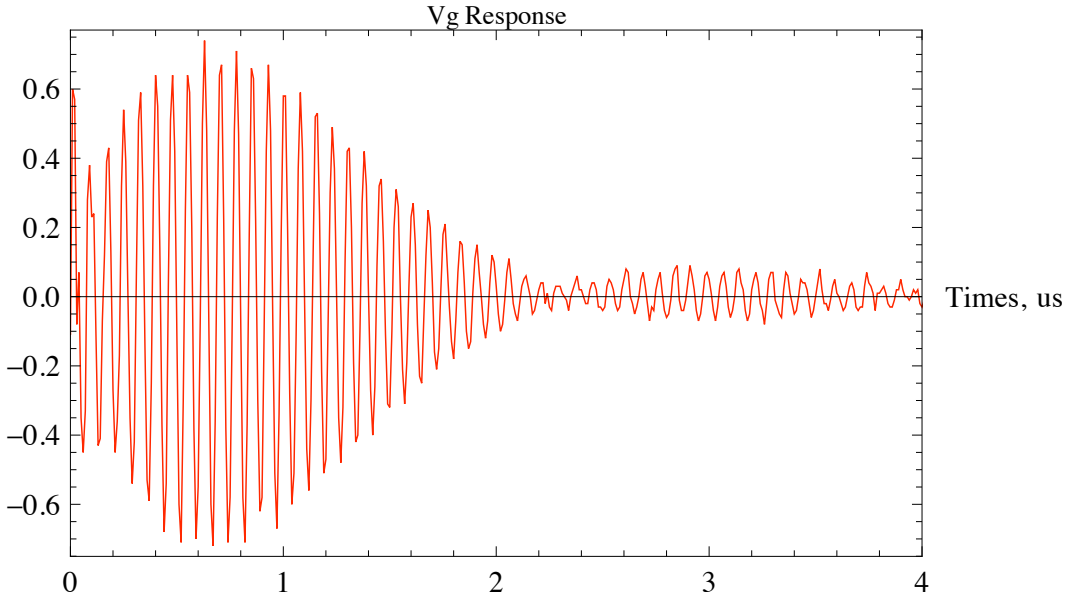

Figure 8. A zoomed in view of the voltage measured over the generator during a sample acceleration pulse performed with a acceleration capacitor charged to 20V.

V. Summary and Concluding Remarks

We have presented a new modification to a FARAD thruster, which will eliminate size and mass costs as well as reduce system complexity. Two technical challenges, protection of the RF generator and adverse affects from the ionization geometry, were described for a Single Stage FARAD thruster. In order to ensure the system would operate safely and efficiently under the new conditions, a circuit was designed which could both protect the RF generator and ensure the initial stored energy is delivered to the SS-FARAD antenna. An analysis was preformed which demonstrated that higher Q resonator would successfully block larger voltage spikes from the RF generator. However, certain high-Q circuits become unfeasible as parasitic effects begin to dominate and detune the circuit. An optimal resonator was determined to utilize a capacitance of no less than 10pF in order to avoid significant problems. For a 13.56 MHz signal, this disallows resonators with Q>20, which is still sufficient to protect the RF generator from a 2kV pulse. If a larger charging voltage is desired, a higher Q circuit could be built under these constraints by using a lower RF frequency to generate the plasma. The 13.56 MHz frequency was chosen for its ubiquity in RF technologies and is not a necessity.

Future work will be designed to explore the second challenge to determine the possible adverse affects from the ionization geometry. While previous attempts to pre-ionize propellant using the acceleration coil has lead to propellant-antenna decoupling prior to the acceleration pulse, the lower voltages and oscillating nature of a RF discharge has the potential to ionize the propellant with little adverse effect. In a future study we will measure the energy required for plasma generation near the antenna coil surface, as well as examine how the propellant moves under the RF generation signal in order to establish whether the RF source can generate a plasma with no decoupling effects that may adversely impact the overall propulsive performance of the accelerator.

Acknowledgments

This research was carried out with support from the Plasma Science and Technology Program from the Princeton Plasma Physics Laboratory. We would like to thank Robert Sorenson for his helpful knowledge of RF systems and 3d renderings.

References

[1]Russell, D., Poylio, J. H., Goldstein, W., Jackson, B., et al. "The Mark VI Pulsed Inductive Thruster." Number AIAA 2004-6054, September 2004.

[2]Lovberg, R. H., Dailey, C. L., "PIT Mark V Design." Number AIAA 1991-3571, September 1991.

[3]Jahn, R. G., *Physics of Electric Propulsion*, McGraw-Hill, New York, 1968.

[4]Polzin, K., "Comprehensive Review of Planar Pulsed Inductive Plasma Thruster Research and Technology," *Journal of Propulsion and Power*, Vol. 27, No. 3, May-June 2011.

[5]Choueiri, E., Polzin, K., "Faraday Accelerator with Radio-frequency Assisted Discharge (FARAD)." *Journal of Propulsion and Power*, Vol. 22, No. 3, May-June 2006.

[6]Polzin, K., PhD Thesis, Mechanical and Aerospace Engineering Dept., Princeton University, 2006.

[7]Hallock, A., Choueiri, E., "Current Sheet Formation in a Conical Theta Pinch FARAD." 30^{th} IEPC 2007-165, September 2007.

[8]Polzin, K., Rose, M. F., Miller, R., "Laboratory-Model Integrated-System FARAD Thruster," 44^{th} Jnt. Prop. Conf. Number AIAA 2008-4821, July 2008.

[9]Hallock, A., Polzin, K., Bonds, K., Emsellem, G., "Effect of Inductive Coil Geometry and Current Sheet Trajectory of a Conical Theta Pinch Pulsed Inductive Plasma Accelerator," 47^{th} Jnt. Prop. Conf. Number AIAA 2011-6068, August 2011.

[10]Hallock, A., et al. "Design of a Microwave Assisted Discharge Inductive Plasma Accelerator." 46^{th} Jnt. Prop. Conf. Number AIAA 2010-6527, July 2010.